

SUPPLEMENTARY MATERIAL

to

Crevasse-induced Rayleigh-wave azimuthal anisotropy on Glacier de la Plaine Morte, Switzerland

Fabian LINDNER,¹ Gabi LASKE,² Fabian WALTER,¹ Adrian K. DORAN²

¹*Laboratory of Hydraulics, Hydrology and Glaciology (VAW), ETH Zürich, Zürich, Switzerland*

²*Institute of Geophysics and Planetary Physics, Scripps Institution of Oceanography, UC San Diego, USA*

Correspondence: Fabian Lindner <lindner@vaw.baug.ethz.ch>

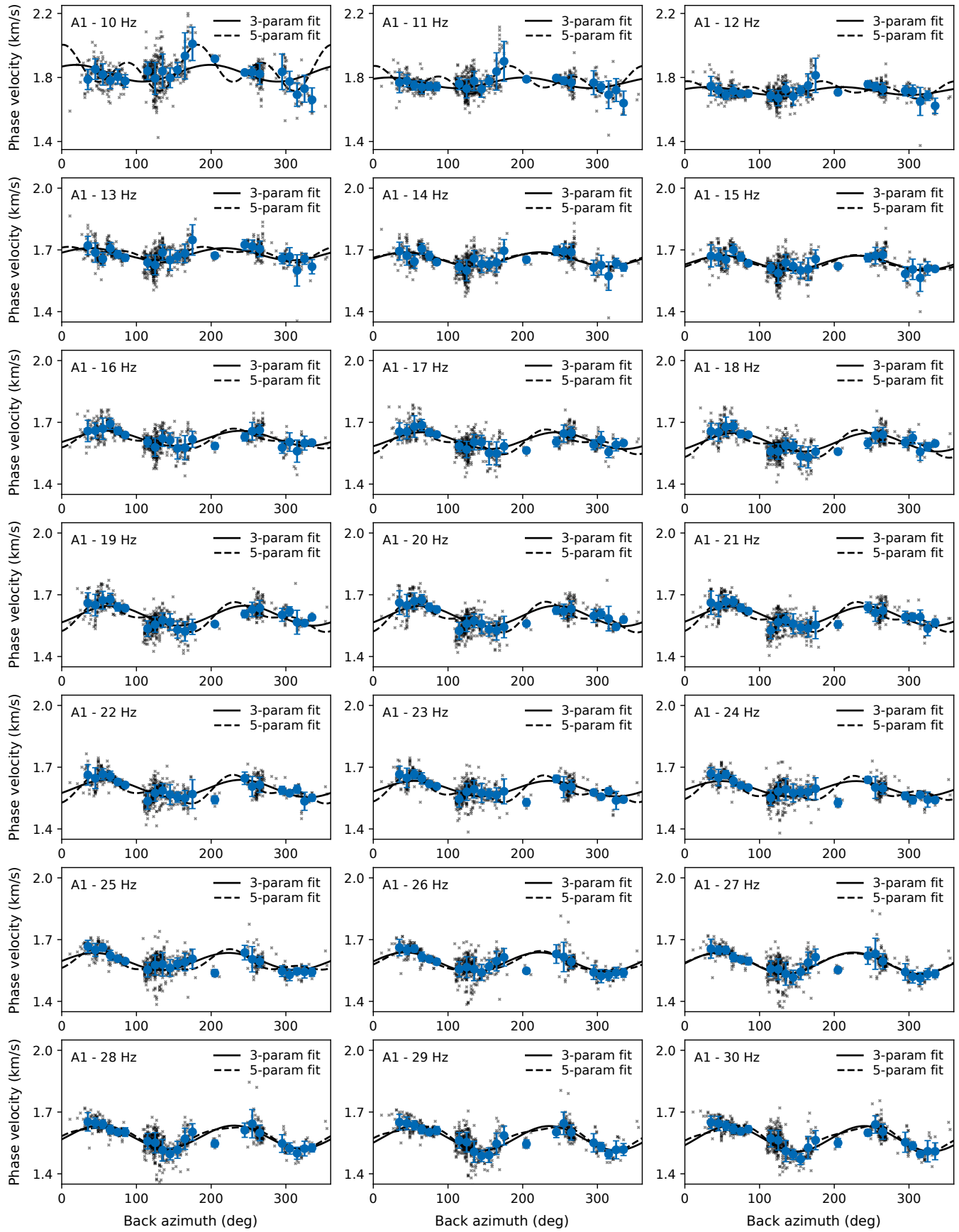


Fig. S1: Phase velocity as a function of back azimuth for array A1. Same as Fig. 5 but for all integer frequencies in the range 10–30 Hz. Note that the phase velocity range is not the same for all frequencies.

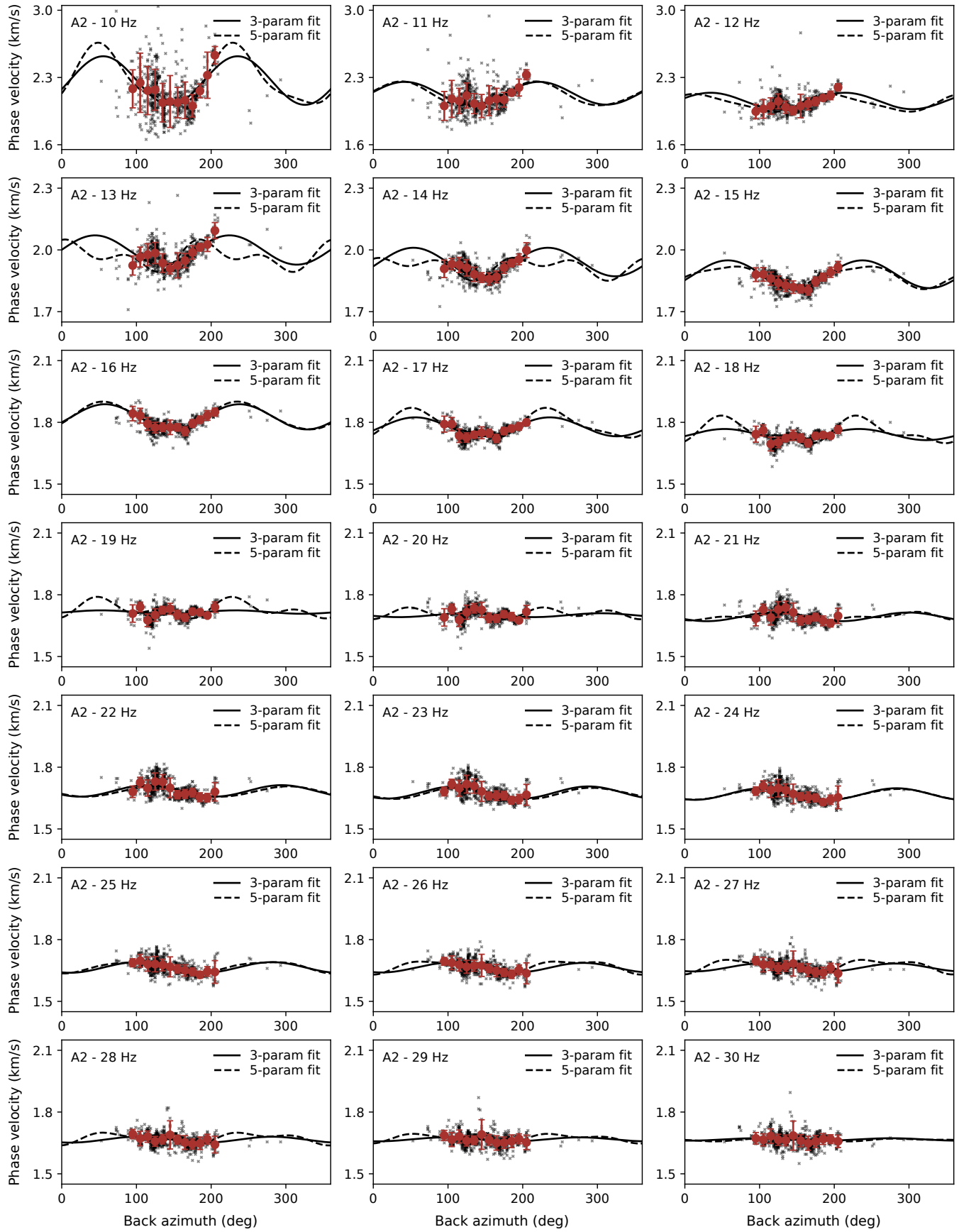


Fig. S2: Phase velocity as a function of back azimuth for array A2. Same as Fig. 5 but for all integer frequencies in the range 10–30 Hz. Note that the phase velocity range is not the same for all frequencies.

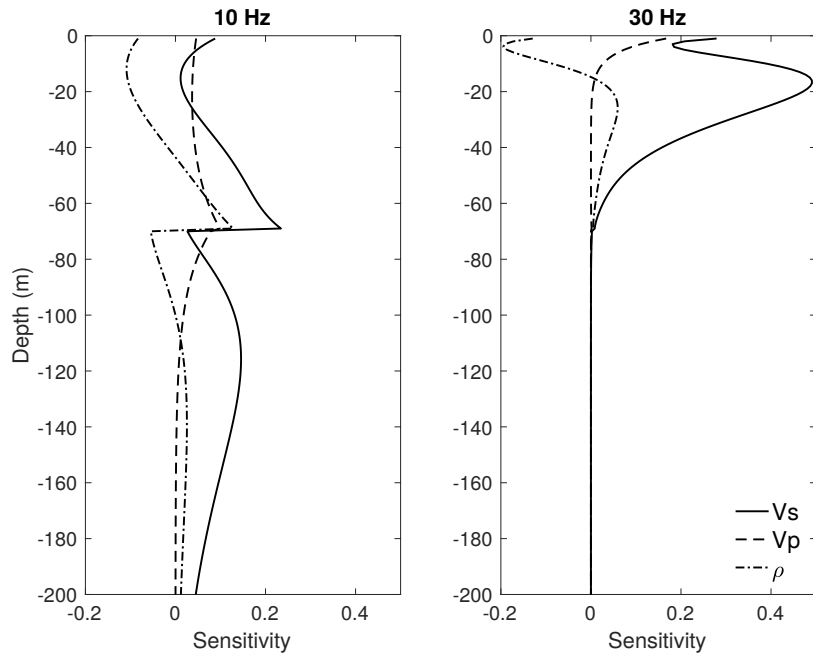


Fig. S3: Rayleigh wave sensitivity kernels at 10 and 30 Hz as suitable for modeling at array A2. The underlying two-layer model consists of 70 meters of ice over a half-space of karst bedrock. The parameters for this model are summarized in Table 1. The kernels were computed using the MATLAB code of Haney and Tsai (2017). While sensitivity of 10-Hz Rayleigh wave phase velocity to basement structure is reduced immediately below the ice-basement boundary, note significant sensitivity to basement structure well below the boundary.

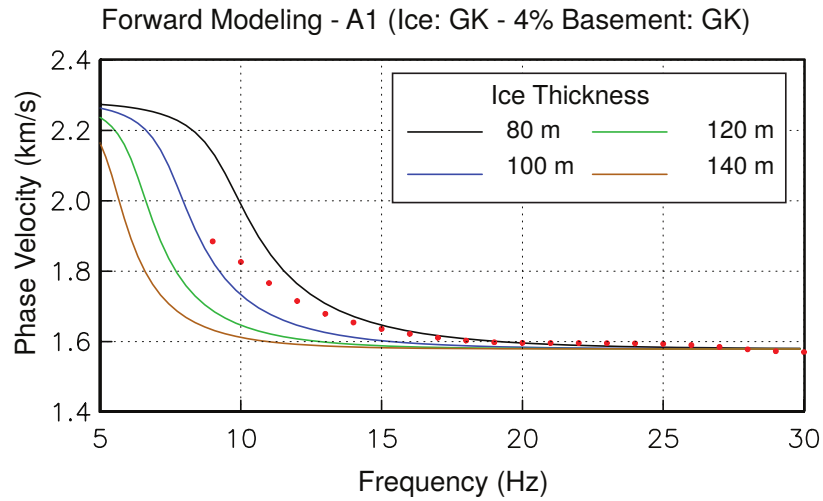


Fig. S4: Forward modeling attempt to fit average phase velocities at array A1. Solid lines with different color mark varying ice thickness. Ice and basement velocities were taken from the GK model though ice velocities and density were 4% lower. Red symbols show the azimuthally averaged phase velocity from Fig. 6

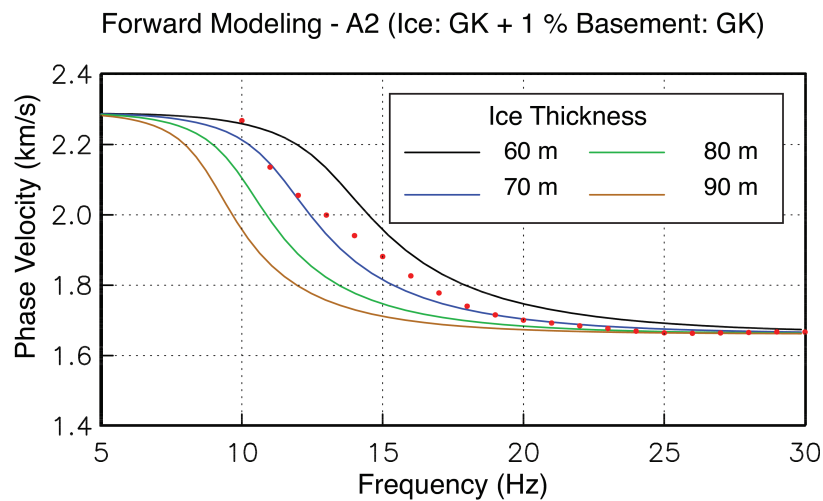


Fig. S5: Forward modeling attempt to fit average phase velocities at array A2. Solid lines with different color mark varying ice thickness. Ice and basement velocities were taken from the GK model though ice velocities and density were 1% higher. Red symbols show the azimuthally averaged phase velocity from Fig. 6

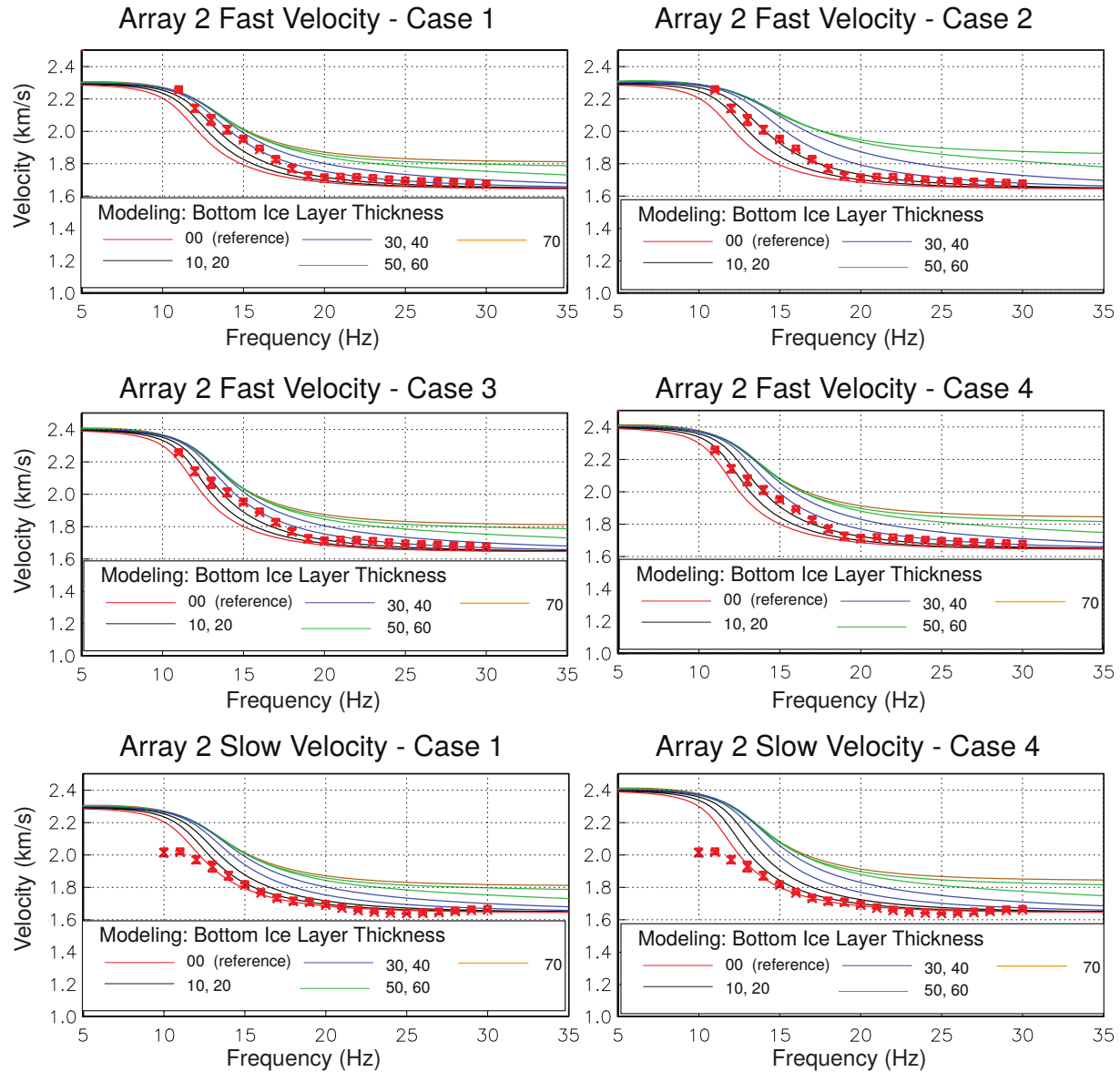


Fig. S6: Forward modeling attempt to fit the fast and slow phase velocities at array A2. The top four panels show fits for the fast phase velocity, the bottom two show the two end-member cases for the slow phase velocity. Solid lines with different color mark the thickness of the faster lower ice layer, according to Table S1. Red symbols show the observed phase velocity from Fig. 9. We conducted four suites of runs with various combinations of higher velocities in the lower ice layer or the basement (cases 1-4, Table S1). All four suites provide very similar fits to the data, demonstrating the existing trade-offs between layer thickness of the bottom ice layer, bottom ice velocity, and basement velocity. Case 1 requires the thickest layer (30 m) to fit the low-frequency data, but data between 18 and 21 Hz require a thinner layer. In case 2, most data follow the predictions for a 20-m thick bottom ice layer, but Vs in this layer exceeds 2000 m/s. In case 3, most data agree with a 10-20-m thick bottom layer but data between 14 and 17 Hz are best fit by a 30-m-thick layer. Case 4 requires a thinner, 15-25-m-thick bottom ice layer. In all cases, the slow phase velocities are best fit using GK ice velocities. The data are equally well fit with either basement velocity, so anisotropy in the basement is not needed to fit both slow and fast phase velocities.

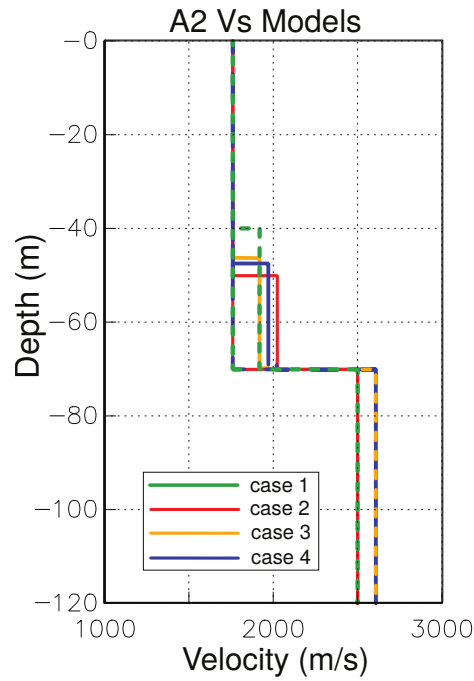


Fig. S7: Resulting models for array A2, for the four cases discussed in Fig. S6. Layer velocities are those in Table S1 but the internal boundary in the ice is approximated according to the discussion of Fig. S6.

Table S1: Forward models for Array A2.

Layer	Thickness (m)	Vp (m/s)	Vs (m/s)	ρ (kg/m ³)	Comment
case 1					
top ice	40–45	3630	1760	910	GK
bottom ice	25–30	3993	1936	1001	GK+10%
bedrock	∞	4500	2500	2500	GK
case 2					
top ice	50	3630	1760	910	GK
bottom ice	20	4175	2024	1074	GK+15%
bedrock	∞	4500	2500	2500	GK
case 3					
top ice	40–55	3630	1760	910	GK
bottom ice	15–30	3993	1936	1001	GK+10%
bedrock	∞	4725	2625	2625	GK+5%
case 4					
top ice	45–55	3630	1760	910	GK
bottom ice	15–25	4066	1971	1019	GK+12%
bedrock	∞	4725	2625	2625	GK+5%

REFERENCES

- Haney MM and Tsai VC (2017) Perturbational and nonperturbational inversion of Rayleigh-wave velocities. *Geophysics*, **82**(3), F15–F28, ISSN 0016-8033 (doi: 10.1190/geo2016-0397.1)